STEM CELLS®

Original Article

Long-Term Survival of Dopamine Neurons Derived from Parthenogenetic Primate Embryonic Stem Cells (Cyno-1) After Transplantation

Rosario Sánchez-Pernaute,[a,b] Lorenz Studer,[c] Daniela Ferrari,[b] Anselme Perrier,[c] Hyojin Lee,[c] Angel Viñuela,[a,b] Ole Isacson[a,b]

[a]McLean Hospital/Harvard University Udall Parkinson's Disease Research Center of Excellence and [b]Neuroregeneration Laboratories, McLean Hospital, Belmont, Massachusetts, USA; [c]Laboratory of Stem Cell & Tumor Biology, Division of Neurosurgery, Memorial Sloan-Kettering Cancer Center, New York, New York, USA

ABSTRACT

Dopamine (DA) neurons can be derived from human and primate embryonic stem (ES) cells in vitro. An ES cell–based replacement therapy for patients with Parkinson's disease requires that in vitro–generated neurons maintain their phenotype in vivo. Other critical issues relate to their proliferative capacity and risk of tumor formation, and the capability of migration and integration in the adult mammalian brain. Neural induction was achieved by coculture of primate parthenogenetic ES cells (Cyno-1) with stromal cells, followed by sequential exposure to midbrain patterning and differentiation factors to favor DA phenotypic specification. Differentiated ES cells were treated with mitomycin C and transplanted into adult immunosuppressed rodents and into a primate (allograft) without immunosuppression. A small percentage of DA neurons survived in both rodent and primate hosts for the entire term of the study (4 and 7 months, respectively). Other neuronal and glial populations derived from Cyno-1 ES cells showed, in vivo, phenotypic characteristics and growth and migration patterns similar to fetal primate transplants, and a majority of cells (>80%) expressed the forebrain transcription factor brain factor 1. No teratoma formation was observed. In this study, we demonstrate long-term survival of DA neurons obtained in vitro from primate ES cells. Optimization of differentiation, cell selection, and cell transfer is required for functional studies of ES-derived DA neurons for future therapeutic applications. STEM CELLS 2005;23:914–922

INTRODUCTION

Embryonic stem (ES) cells provide an unlimited source of cells that can be tailored to meet specific criteria for cell-replacement therapies. ES cell lines have been derived from human [1] and nonhuman primate blastocysts, including parthenogenetic primate blastocysts, [2, 3]. Neuronal and glial cell lineages have been derived in vitro from these primate and human ES cell lines [4, 5] and examined in vivo in transplantation paradigms [5–7]. However, a number of critical questions remain to be addressed to develop an ES cell–based therapy for neurodegenerative disorders, in particular for Parkinson's disease (PD). These questions relate to survival and proliferation, stability of neuronal phenotypes induced in vitro, and capacity of synaptic integration and are therefore a prerequisite for investigation of functional potential.

The Cyno-1 cell line used in this study was derived from the inner cell mass of a parthenogenetic blastocyst and has similar characteristics to normal fertilization–derived primate ES cells [3]. Dopamine (DA) neurons have been derived in vitro from this cell line [3]. Neural precursors derived from mouse ES cells [8] can be directed into defined neuronal phenotypes by the timed

exposure to factors that control antero-posterior and dorso-ventral fate specification during normal development in vivo, including fibroblast growth factors (FGF) 4 and 8, retinoic acid, and sonic hedgehog (SHH) [9]. To obtain DA neurons from primate ES cells in this study, we first used a stromal cell feeder coculture system for neural induction [6, 10, 11], followed by the sequential exposure to inductive signals, such as SHH and FGF8, that control DA specification during embryogenesis [12] and factors that promote DA neuron differentiation and maturation. In this study, transplantation of in vitro differentiated Cyno-1 cells was performed into adult immunosuppressed rats and into the primate striatum (allograft) without immunosuppression.

MATERIALS AND METHODS

Cell Culture and In Vitro Characterization

All the experiments were performed using a nonhuman primate cell line [2]. Cyno-1 is a line of primate (*Macaca fascicularis*) stem cells derived from the inner cell mass of a parthenogenetic blastocyst. Undifferentiated Cyno-1 cells exhibit high telomerase activity and are positive for primate ES cell markers, such as alkaline phosphatase activity, octamer binding transcription factor 4 (Oct-4), stage-specific embryonic antigen 4 (SSEA-4), and tumor rejection antigens (TRAs) 1–60 and 1–81, and have a normal karyotype [3]. These cells can be maintained in vitro in an undifferentiated state for at least 2 years and can be induced to differentiate into neurons under appropriate culture conditions [2, 3]. Neural differentiation of Cyno-1 cells was induced by coculture on the stromal feeder cell line MS5 or on transgenic MS5 cells that stably overexpress Wnt1 after transfection (Fugene-6) of a Wnt1 expression construct, followed by G418 selection. MS5 and MS5-Wnt were maintained in α-minimum essential medium containing 10% fetal bovine serum and 2 mM L-glutamine, as described previously [10]. Cyno-1 cells were plated at a density of 250–1,000 cells per cm^2 on a confluent layer of irradiated (50 Gy) stromal cells in 6-cm cell-culture plates in serum replacement medium (SRM) containing Dulbecco's minimal Eagle's medium, 15% knockout serum replacement (KSR; Invitrogen, Carlsbad, CA, http://www.invitrogen.com), 2 mM L-glutamine, and 10 µM mercaptoethanol. After 12 days in SRM, cultures were switched to N2 medium modified according to [13]. Medium was changed every 2–3 days, and growth factors were added in various combinations as shown in Figure 1A: sonic hedgehog (SHH; 200 ng/ml), fibroblast growth factor 8 (FGF8; 100 ng/ml), brain-derived neurotropic factor (BDNF; 20 ng/ml), glial-derived neurotropic factor (GDNF; 10–20 ng/ml), and transforming growth factor β3 (TGFβ3; 1 ng/ml), all from R&D Systems (Minneapolis, http://www.rndsystems.com); dbcAMP (0.5–1 mM) and ascorbic acid (AA) (0.2 mM) from Sigma-Aldrich (St. Louis, http://www.sigmaaldrich.com).

Rosettes structures were harvested mechanically from feeders at day 21 of differentiation and replated on polyornithine (15 µg/ml)/laminin (1 µg/ml)–coated culture dishes in N2 medium supplemented with SHH, FGF8, AA, and BDNF (Passage 1). After 7–9 days (80% confluency), cells exposed to SHH and FGF8 were mechanically passaged after exposure to Ca^2/Mg^2-free Hanks' balanced saline solution (HBSS) for 1 hour at room temperature and spun at 200g for 5 minutes. Cells were resuspended in N2 medium replated onto polyornithine/laminin-coated culture dishes ($50–100 \times 10^3$ cells/cm^2) in the presence of SHH, FGF8, AA, and BDNF (Passage 2). After an additional 7–9 days of culture, cells were differentiated in the absence of SHH and FGF8, in the final differentiation medium containing BDNF, GDNF, TGFβ3, dbcAMP, and AA.

Cell Preparation and Transplantation Procedures

Cells were treated with mitomycin C (1 µg/ml) for 90 minutes at 37°C, harvested without enzymatic digestion, and mechanically dissociated into a cell suspension. Acridine orange/ethidium bromide staining was used to assess cell viability. Cells were counted and resuspended at 100,000 viable cells per µl in N2 supplemented media. The same cell suspension was used for rat (further diluted to 25,000 cells/µl) and for the primate transplantation (see below) and replated for further characterization (supplemental online Fig. 1).

Animal Procedures

All animal procedures were performed in accordance with National Institutes of Health guidelines and were approved by the Animal Care and Use Committee at McLean Hospital and Harvard Medical School.

Rodent Transplantation

6-Hydroxydopamine–lesioned female Sprague-Dawley rats (200–250 g) were purchased from Charles River Laboratories (Wilmington, MA, http://www.criver.com) or Taconic (Germantown, NY, http://www.taconic.com), and housed under standard conditions, 2 to 3 per cage in the animal facility at McLean Hospital. Transplantation was performed as previously described [14, 15]. To prevent rejection of grafted primate cells, rats were immunosuppressed with cyclosporin A (15 mg/kg per day, Sandimmune; Sandoz, East Hanover, NJ, http://www.sandoz.com) starting 1 day prior to surgery. After 10 weeks, the dosage of cyclosporin was reduced to 10 mg/kg per day. At different time points after implantation, animals were anesthetized by an i.p. overdose of pentobarbital (150 mg/kg), and perfused intracardially with 70 ml heparinized saline (0.1% heparin in 0.9% saline) followed by 100 ml paraformaldehyde (4% in PBS). Brains were removed, postfixed for 4 hours in 4% paraformaldehyde, equilibrated in sucrose (20% in PBS), and sectioned on a freezing microtome in 40-µm slices that were serially collected.

Primate Transplantation

A 6-year-old male cynomolgus monkey received weekly i.v. injections of 1-methyl, 4-phenyl, 1,2,3,6-tetrahydropyridine (MPTP) (0.3 mg/kg per week for 16 weeks, total dosage 13.6 mg) that resulted in mild stable parkinsonism (Parkinsonian Rating Scale [PRS] score = 9.3. [total score from 0–24]). The last MPTP injection was performed 13 months before transplantation. Transplantation sites were defined using e-film version 1.8.3 (Merge eFilm, Milwaukee, http://www.merge.com) on coronal MR T2 images of the monkey brain obtained with the animal placed in the same stereotactic frame used for the surgery. Two sites were defined in the right putamen: anterior, at the level of the anterior commissure (AC –1 mm), and posterior, in the postcommissural putamen (AC –4 mm). Surgery was performed in sterile conditions under isoflurane anesthesia with assisted ventilation. After cranial preparation, a skin incision was made over the target area, and skin, muscle, and fascia were retracted to expose the cranial surface. A burr-hole was drilled over the target area, and 25 µl of the cell suspension were slowly injected along 4 mm (–20 to –16 mm ventral from the dura) at each antero-posterior site, using a blunt tip needle with two side-holes [16]. After completion of injections, the surgical site was washed, the burrhole sealed with bone wax, and the fascia, muscle, and skin were sutured in planes. The animal received cephazolin (20 mg/kg per 12 hour i.m.) and dexamethasone (1 mg/day i.m.) for 5 days and analgesia (buprenorphine 0.005 mg/kg per 12 hour i.m.) for 3 days. No cyclosporine was given. The animal showed no complications. Motor scores and tests were performed biweekly. Seven months after the transplant, the animal was sedated with ketamine (15 mg/kg) and anesthetized with pentobarbital (Nembutal; 25 mg/kg, i.v.) and perfused transcardially with ice-cold heparinized saline followed by 4% paraformaldehyde. The brain was postfixed overnight and equilibrated in graded sucrose solutions (10%–30% in PBS) and sectioned on a freezing microtome in 40-µm slices that were serially collected.

Histological and Stereological Procedures

Immunohistochemistry was performed on free-floating coronal sections, as previously described [14, 15].

Donor cells were identified in the rodent by using two primate-specific antibodies: human nuclear antigen (HNA) (1:50; Chemicon, Temecula, CA, http://www.chemicon.com) and a primate-specific neural cell adhesion molecule (NCAM) (clone eric1, 1:100; Santa Cruz Biotechnology, Santa Cruz, CA, http://www.scbt.com). Characterization of the grafted cell phenotypes was performed using multiple immunofluorescence labeling with the following primary antibodies: nestin (rat 401, 1 µg/ml) and engrailed-1 (clone 4G11; 1:20) (purchased from the Developmental Studies Hybridoma Bank, Iowa City, IA, http://www.uiowa.edu/~dshbwww); glial fibrillary acidic protein (GFAP) (1:500; DakoCytomation, Carpinteria, CA, http://www.dakocytomation.

us); O4 (1:50), neuronal nuclei (NeuN) (1:250), aromatic amino acid decarboxylase (AADC) (1:250), and DA transporter (DAT) (1:1,000) (Chemicon); Oct-4 (1:100) and doublecortin (Dcx) (1:250) (Santa Cruz Biotechnology); tyrosine hydroxylase (TH) (1:250), vesicular monoamine transporter (VMAT)-2 (1:250), and DA beta hydroxylase (DBH) (primate specific,1:250) (Pel-Freez Biologics, Rogers, AR, http://www.dynalbiotech.com); Serotonin (5HT) (1:5,000; DiaSorin, Stillwater, MN, http://www.diasorin.com); calbindin -D28k (1:1,000) and calretinin (1:1,000) (Swant, Bellinzona, Switzerland, http://www.swant.com); brain factor1 (Bf1) (polyclonal, 1:500) (gift from Dr Lai); and Pax2 and neuron-specific class III β-tubulin (clone TuJ1; 1:1,000) (Covance, Berkeley, CA, http://www.covance.com). Sections were permeabilized with 0.1% Triton X-100 and incubated with primary antibodies in 10% normal serum overnight; after rinsing, sections were incubated in fluorescence-labeled secondary antibodies (Molecular Probes, Eugene, OR, http://probes.invitrogen.com) for 1 hour at room temperature, rinsed, and incubated with Hoechst 33342 (4 µg/ml). For light microscopy, biotinylated secondary antibody (1:300; Vector Laboratories, Burlingame, CA, http://www.vectorlabs.com) was used, followed by incubation in streptavidin-biotin complex (Vectastain ABC Kit Elite, Vector Laboratories) for 60 minutes at room temperature and visualized by incubation in 3,3'-diaminobenzidine (DAB) solution with nickel enhancement (Vector Laboratories). For detection of proliferating cell nuclear antigen (PCNA) (1:100; Santa Cruz Biotechnology), antigen retrieval was performed by preincubating the sections in target retrieval solution (DakoCytomation) for 20 minutes at 85°C. Control experiments were performed by omission of primary antibodies and using different combination of secondary antibodies. Confocal analysis was performed using a Zeiss LSM510/Meta station (Thornwood, NY, http://www.zeiss.com). Qualitative analysis was performed by systematic evaluation of a series of sections spanning the grafts. For identification of signal colocalization within a cell, optical sections were kept to a minimal thickness, and orthogonal reconstructions were obtained. Design-based stereology was performed on the sections using Stereo Investigator image-capture equipment and software (MicroBrightField, Williston, VT, http://www.microbrightfield.com). Graft volumes were calculated using the Cavalieri estimator probe. The coefficient of error was used to assess probe accuracy, and $p < .05$ was considered acceptable. Graft maps and contours were generated using Neurolucida virtual slice and tracing software (MicroBrightField, Williston, VT, http://www.microbrightfield.com). Cell counts of TH-positive and 5HT-positive neurons were performed on every sixth section, using an Axioplan microscope (Zeiss, Thornwood, NY, http://www.zeiss.com) with a ×40 lens. Only stained cells with visible dendrites were counted as TH-positive neurons, and the cell counts from serial sections were corrected and extrapolated for whole graft volumes, using the Abercrombie method [17]. Estimation of

ubiquitously expressed markers (NeuN, Bf1) was assessed in random fields in all available sections containing the graft within one series (at least 1,000 cells), and results were expressed as percentages. Cell density outside the graft was estimated on serial sections stained for HNA, using a semiquantitative scale (<10, 10–50, 50–100, 100–1,000, >1,000) on the following anatomical regions: striatum, external capsule, forceps maior and genu of the corpus callosum, anterior commissure, and cortex. Data are presented as mean ± SEM. Student t-tests were performed to evaluate treatment effects in the mitomycin C experiment (supplemental online Fig. 2). Simple regression analyses were performed to evaluate correlation between volumes and cell density and types. Statistical analyses were made using Statview software (SAS Institute Inc., Cary, NC, http://www.sas.com).

RESULTS

Transplantation of Differentiated Primate ES Cells into the Rat Striatum

In this protocol for in vitro neuronal differentiation (Fig. 1A), undifferentiated Cyno-1 cells (Fig. 1B) on MS5 or MS5-wnt1 feeder cells formed neural rosettes within 10–14 days (Fig. 1C). After replating on coated (feeder-free) dishes, neural rosettes were exposed to a second induction phase with SHH and FGF8 (Fig. 1A) which resulted in neuronal differentiation (Fig. 1D) and expression of Pax2 (day 28, not shown) followed by engrailed 1 (Fig. 1E) in 20% of the cells at the end of passage 2 expansion (day 35). Upon differentiation of passage 2 cells for 7 more days in the absence of SHH and FGF8 and in the presence of various trophic factors (Fig. 1A), 30%–60% of the cells expressed neuronal markers (TuJ-1), and up to 70% of these neurons coexpressed TH (Figs. 1F, 1G). These cells were briefly exposed to fresh mitomycin C immediately before being harvested and dissociated into a cell suspension for grafting. We previously determined the effect of mitomycin C on graft size and proliferation 3 weeks after transplantation (see below and supplemental online Fig. 2). Some cells were replated in differentiation media and fixed 3, 5, and 12 days later for control of mitomycin C and cell-preparation effect (supplemental online Fig. 1). The replated cells formed small clusters in which the majority of cells were nestin or TuJ1-positive; 2%–3% of the TuJ1-positive cells were TH, and 10% were Bf1-positive cells (not shown); these percentages were similar at 5 and 12 days. Although these may not correspond exactly to the com-
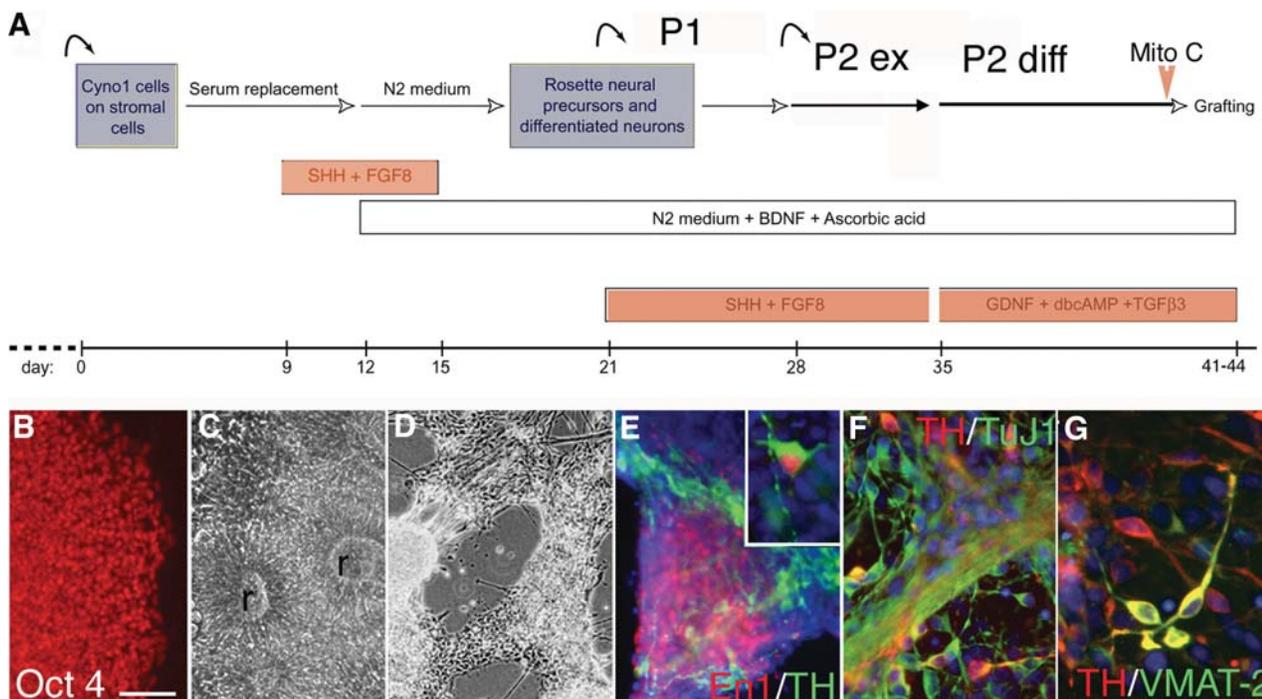

Figure 1. In vitro differentiation of primate ES cells. **(A):** Schematic representation of the sequential steps designed to induce a dopamine neuronal phenotype from undifferentiated primate ES cells. ES cells are first grown in a coculture system on stromal feeders. At the rosette stage, these neuroepithelial structures are replated on coated dishes in a feeder-free system for differentiation. **(B–D):** Microscopic images illustrating the aspect of the colonies at each passage. Undifferentiated stage Cyno-1 cells grow in colonies and all cells **(B)** express the transcription factor Oct-4. **(C):** Soon after the first passage, cells are organized into typical neuroepithelial structures (rosettes, r); **(D):** At the differentiation stage neurons grow in clusters and extend out neurites and **(E)** express midbrain genes like Engrailed-1 (En1), which is colocalized in some neurons with TH. **(F):** TH neurons coexpressed the neuronal marker β-tubulin III (clone TuJ1) and **(G)** some coexpressed VMAT-2 (yellow coexpression). Scale bars = 100 μm **(B–C)**, 150 μm **(D)**, 75 μm **(E)**, 50 μm **(F)**, 35 μm **(G)** and inset in **(E)**. Abbreviations: BDNF, brain-derived neurotropic factor; ES, embryonic stem; FGF8, fibroblast growth factor 8; GDNF, glial-derived neurotropic factor; TH, tyrosine hydroxylase; SHH, sonic hedgehog; TGFβ3, transforming growth factor β3; TH, tyrosine hydroxylase; VMAT, vesicular monoamine transporter.

position of the population in the cell suspension, due to the effect of culture conditions upon replating, such as cell density and media, these data suggest that TH-positive cells are particularly sensitive to dissociation and replating compared with the overall neuronal population within the grafted cell suspension.

We transplanted these differentiated ES cells into rats ($n = 7$) and into one primate (see below). Rat brains were examined 16 weeks post-transplantation; six animals had surviving grafts. Graft volumes were small (2.32 ± 0.6 mm^3), and PCNA expression in the graft core was low (supplemental online Fig. 2C). TH-positive neurons were found in all the grafts close to the host-graft interface (Figs. 2B, 2C) in a typical peripheral distribution around the core of the graft, which was strongly immunoreactive for double-cortin (Dcx, not shown), a neurofilament associated protein highly expressed by young and migrating neuroblasts, which is expressed only in neurogenic regions in the adult host brain. The TH-positive neurons in the graft were HNA-positive (Fig. 2D), DBH-negative, and calbindin-negative (not shown); some cell bodies and fibers expressed AADC and the transporters DAT and VMAT-2 (Figs. 2E–2H). DAT expression was observed in TH fibers projecting into the host (Fig. 2F). TH cell numbers in the grafts (557 ± 117, $n = 6$)
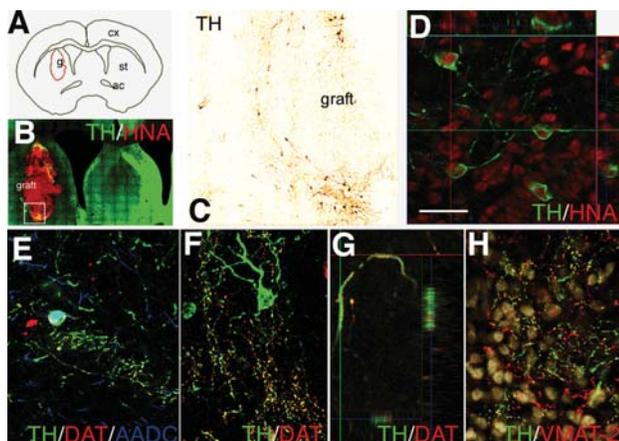
were directly correlated with the graft volume ($R^2 = 0.91$, $p < 0.01$) and inversely correlated with the percentage of cells expressing the forebrain marker Bf1 ($R^2 = 0.89$, $p < 0.01$). Most of the HNA-positive cells in the core of the grafts expressed NeuN (Fig. 3B) and were positive for the forebrain transcription factor Bf1 ($83\% \pm 4\%$, not shown). 5HT neurons (not shown) were present in the grafts in lower numbers (65 ± 19, 1:5 TH-positive). At 16 weeks, many primate (HNA-positive) cells were found away from the core of the graft (Fig. 3), mainly in the ipsilateral striatum and also along the corpus callosum and the anterior commissure, reaching the contra-lateral hemisphere. Semiquantitative estimation of HNA-positive cell density (Fig. 3A) showed a gradient away from the graft. Many of these cells away from the core expressed Dcx (some organized in migratory chains, Fig. 3G) or, in white matter tracts, glial markers (GFAP and O4, Figs. 3D–3F), and few were NeuN-positive, which were located in close proximity to the graft core. There were some HNA-positive cells in the subventricular zone (SVZ) (Fig. 3H), which were GFAP-negative and either positive or negative for Dcx.
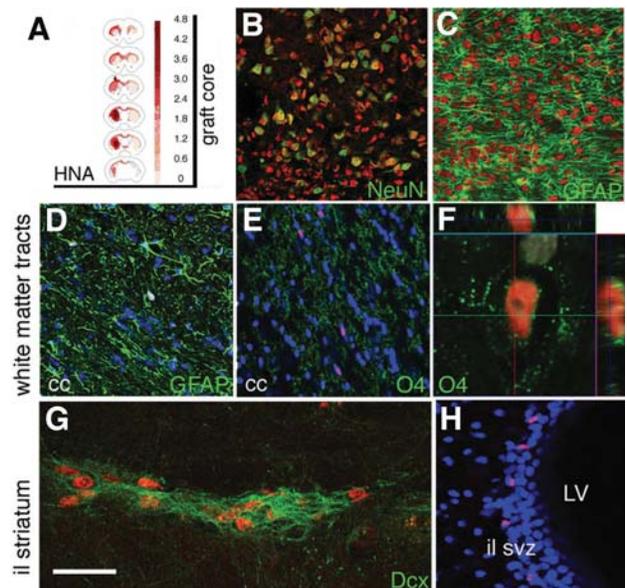

Figure 2. Grafted cells were identified by HNA expression **(B–D)** 4 months post-transplantation into the rat striatum. **(A):** Computer-generated graft contour and **(B)** virtual slice acquired on a representative coronal section double immunostained for TH and HNA. The boxed area is shown in **(B)**. TH-positive neurons derived from primate ES cells were **(B)** located at the periphery of the grafts and **(C)** showed nuclear expression of the primate and human specific marker HNA, as shown in **(D)** in a confocal reconstruction. **(E, F):** TH neurons in the grafts expressed AADC **(E)** and some TH-positive neurites expressed DAT **(E–G)**. In **(G)** DAT and TH coexpression is shown in a 3-D reconstruction of a confocal z-stack through a DA fiber. **(H):** VMAT-2 was expressed in TH-positive and -negative (presumably serotonergic) fibers. Scale bars = 2 mm **(A)**, 250 µm **(B)**, 100 µm **(C)**, 30 µm **(D–F, H)**, and 10 µm **(G)**. Abbreviations: AADC, aromatic amino acid decarboxylase; ac, anterior commisure; cx, cortex; DA, dopamine; DAT, dopamine transporter; ES, embryonic stem; g, graft; HNA, human nuclear antigen; st, striatum; TH, tyrosine hydroxylase; VMAT, vesicular monoamine transporter.

Figure 3. Primate HNA-positive cells (HNA is shown in red in all panels) migrated away from the graft core 4 months post-transplantation into the rat striatum. **(A):** Semiquantitative estimation of HNA-positive cell density was performed on serial sections, and the average density for the 6 grafted animals is shown on representative coronal sections (see Materials and Methods). **(B, C):** In the graft core, most HNA-positive cells expressed **(B)** NeuN, and not **(C)** GFAP. **(D, F):** HNA-positive glial cells were found along white matter tracts: astrocytes [GFAP-positive in **(D)**] and oligodendrocytes [O4-positive in **(E, F)**] were observed along the corpus callosum. Outside the core of the graft there were some Dcx-positive neuroblasts in chain formations. **(H):** Some HNA-positive cells were found in the SVZ ipsilateral to the graft. Nuclear counterstain (Hoechst) is shown in blue in **(D)**, **(E)**, and **(H)**, and white in **(F)**. Scale bars = 100 µm **(B–E)**, 15 µm **(F)**, 30 µm **(G)**, and 75 µm **(H)**. Abbreviations: GFAP, glial fibrillary acidic protein; HNA, human nuclear antigen; il, ipsilateral to the graft; LV, lateral ventricle; SVZ, subventricular zone.

Transplantation of Differentiated Primate ES Cells into the Primate Striatum

Cells from the same preparation were transplanted into the right postcommissural putamen of a cynomolgus monkey. In this case (allograft), the animal did not receive immunosuppression. Motor scores were evaluated weekly and did not show any asymmetry up to 7 months post-transplantation. Because in this model parkinsonian signs are bilateral and symmetric and the transplant was unilateral, the absence of motor asymmetry is consistent with neither positive nor adverse effects of the grafts. Macroscopic examination of the brain disclosed two grafts at the sites of the injections. The graft volumes were 14 mm^3 for the anterior deposit and 5.4 mm^3 for the posterior graft (Fig. 4A). The grafts were homogeneous and had a slightly higher cell density than the host (Figs. 4D, 4F, 4H). There were no regions of non-neural differentiation, and the grafts did not displace or compress the striatal host parenchyma. Numerous TH-positive cells were located predominantly in the periphery of the graft cores (Figs. 4A, 4B), in a similar arrangement and morphology seen for TH/HNA-positive cells found in the rodent brain (Figs. 2B, 2C). Stereological counts of TH-positive cells showed 2,440 positive cells in the anterior and 880 in the posterior graft (thus, TH cells in vivo were 0.1% of grafted cells). Many of these TH neurons coexpressed AADC (Fig. 4E). As shown in the rodent grafts (Figs. 2E, 2F), some TH fibers within and close to the graft coexpressed DAT (Fig. 4E), but DAT immunoreactivity was not observed in the cell bodies. The grafts contained many NeuN-positive neurons (Figs. 4D, 4F) that coexpressed Bf1 (Fig. 4F). As in the rodent grafts, few neurons in these grafts expressed 5HT (not shown). Clusters of calretinin-positive neurons and some calbindin-positive neurons were observed within the grafts (Fig. 4G). Dcx expression was not detected in the graft core, in contrast with the widespread immunoreactivity for this marker observed in the core in rodent grafts at 4 months. Nevertheless, some Dcx-positive neuroblasts were observed in the primate grafts forming chains (Fig. 4H) reminiscent of those found in the rodents away from the graft core (Fig. 3G). The blood vessels located in the proximity of the grafts showed some perivascular cuffing with strong PCNA positivity, and microglial (CD68-positive) cells were observed in these areas (Fig. 4I).

DISCUSSION

Neurons Derived from Primate Cyno-1 ES Cells Maintain a Stable Phenotype In Vivo

Our findings demonstrate that specific mature neuronal populations that survive several months in the adult rat and primate brain can be generated in vitro from parthenogenetic primate ES cells. We first developed and optimized a protocol for controlled and effective differentiation of primate ES cells into stable neuronal populations suitable for transplantation. During development,

regional neural specification defines neurotransmitter phenotype and neurotrophic factor sensitivity and is controlled by homeodomain proteins [18]. At the midbrain-hindbrain boundary, FGF8 and Wnt1 are necessary for a correct patterning of the midbrain, whereas SHH induces ventral specification [15, 19]. This in vitro protocol was designed to enrich for midbrain DA neurons
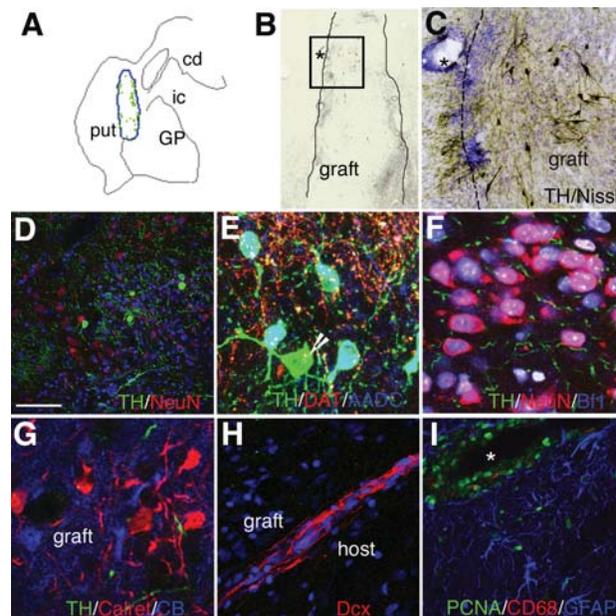

Figure 4. Transplantation of DA cells derived from Cyno-1 ES cells into the primate putamen. (**A**): Computer-generated outline of the graft in the postcommissural putamen and map of the distribution of TH-positive neurons on a representative coronal section. Each green dot represents a TH cell. (**B**): Low power microphotograph of a graft, the boxed area is shown in (**C**) and the asterisks mark the same blood vessel in both images. Clusters of TH-positive cells (the DAB product appears dark brown) were located close to the graft-host interface, where there was a higher nuclear density and higher density of TH-positive fibers (**C, D**) than in the graft core; (**E**) many TH-positive cells in the grafts coexpressed AADC [(**D**), coexpression appears cyan] but not all [arrow in (**D**) points to a TH-positive, AADC-negative cell] and coexpressed the DAT in neurites but not in the cell bodies. (**F, G**): The graft core was predominantly neuronal (NeuN-positive) with most neurons coexpressing Bf1 (coexpression with NeuN appears pink in (**F**). Clusters of neurons inside the graft expressed calretinin (**G**) and calbindin [CB, (**G**)]. Although the morphology of the neurons inside and outside the graft was the same, neurons within the graft were closer to each other than in the host striatum. (**H**): Dcx-positive neuroblasts in a chain-like formation (see also Fig. 3). (**I**): PCNA-positive cells within and close to the graft were mainly located in perivascular spaces and some corresponded to microglia (CD68-positive) and astroglia (GFAP-positive). Scale bars = 2.5 mm (**A**), 125 μm (**B**), 100 μm (**C**), 20 μm (**D–G**), 50 μm (**H**) and (**I**). Nuclear counterstain (Hoechst) is shown in blue in (**D**) and (**H**) and in white in (**F**). * represents blood vessel. Abbreviations: AADC, aromatic amino acid decarboxylase; cd, caudate nucleus; DA, dopamine; DAB, 3,3′-diaminobenzidine; DAT, dopamine transporter; ES, embryonic stem; GFAP, glial fibrillary acidic protein; GP, globus pallidus; ic, internal capsule; PCNA, proliferating cell nuclear antigen; put, putamen; TH, tyrosine hydroxylase.

by reproducing the sequential exposure to ventral and anterior specification signals known to interact at the midbrain–hindbrain neural organizer to induce a midbrain specification [19–22]. The majority of developmental studies of midbrain neuronal populations have been performed in chicks and mice, and there are constitutive differences between rodent and primate normal neural development [23] and ES cell biology [24]. We therefore performed several modifications to adjust the in vitro conditions to the slower developmental pace of primate cells and to reduce the presence of proliferative neural progenitors and were able to generate in vitro DA neurons, which retained a stable midbrain phenotype several months after transplantation. Previous inductive protocols and paradigms, in particular using fetal cells from the forebrain or adult stem cells, have resulted in a transient induction of TH in vitro that is not maintained after transplantation [14, 25–27]. Such protocols typically result also in a predominantly glial differentiation in vivo [28, 29]. Sixteen weeks post-transplantation, TH neurons in the grafts were located in the periphery of the core, in a typical disposition consistently observed in grafts derived from fetal ventral midbrain where TH neurons tend to arrange themselves around the outer perimeter of the grafts [30]. TH neurons grown in vitro appear to be quite vulnerable to harvesting and transplantation procedures [27]. Two recent studies [31, 32] have shown in vivo survival of DA neurons derived from primate and human ES cells using different in vitro and grafting protocols. However, DA survival (and/or in vivo differentiation [31]) and motor benefit in these studies were also limited, suggesting that several factors contribute to poor in vivo outcome. In our study, the grafts did not modify motor asymmetry, probably due to the insufficient number of surviving TH neurons and their limited axonal outgrowth.

Other cells derived from Cyno-1 ES differentiated in vitro resembled fetal forebrain primary cells [33, 34] and forebrain neural stem cells [29, 35]. The differentiation protocol was designed to enhance the DA phenotype (anterior midbrain), but we found that in vivo the majority of the neurons in the grafts (83%) expressed Bf1, a forebrain marker (85% in a previous experiment without mitomycin C, not shown). This predominance can be the result of enhanced forebrain differentiation of progenitors and/or longer expansion of this population dependent on their primate origin [23], since we have not observed this tendency in our transplantation studies using rodent ES cells ([15] and unpublished observations). During embryogenesis, a limited number of diffusible factors signaling at different times and through different regions of the neural tube are combined to specify different neuronal and glial populations [19, 36], and FGF8 from the anterior neural ridge is sufficient to induce forebrain specification, where SHH also induces ventral specification [15, 19]. It is therefore possible that the same signals we used to induce ventral midbrain specification, SHH and FGF8, act in a temporal sequence to induce a (ventral) forebrain phenotype and that this population expands more easily in an appropriate environment, and also due to its primate origin. During development there is a progressive restriction in the cell types that a progenitor can produce: they can produce cells generated at later, but not earlier, stages [37, 38]. Both the extracellular and the intracellular context influence the cell types derived from progenitors and stem cells [39]. An inductive effect of the environment on phenotype specification has been reported in transplantation experiments using fetal and adult stem cells that, nevertheless, appear to retain at least partly their original regional specification [40]. In particular, the expression of later markers of regional identity seems to depend on inductive signals provided by the local environment [41]. However, it is unlikely that uncommitted neural progenitors derived from primate ES cells in our cell culture system adopted the regional fate of the region where they are transplanted.

After 16 weeks, we observed significant migration of glial and neuroblasts (Dcx-positive cells) sometimes forming chains away from the graft core in the rat and primate brain. Typical migratory chains of Dcx-positive neuroblasts were similar to those observed in the neurogenic SVZ and in the rostral migratory stream in the adult brain of rodent [42–44] and macaque [45]. Interestingly, we observed a small number of HNA-positive cells in the SVZ, suggesting a homing effect of neural stem cells to their structural "niche" in the SVZ, analogous to that of hemopoietic stem cells to the bone marrow [46]. The niche maintains stem cells in a relatively quiescent state, and therefore presence and growth of these stem cells should not be viewed as tumoral or unregulated proliferation. It would be interesting to identify the signals guiding migration and adhesive interactions of neural stem/progenitors and neuroblasts in the niche [47] in the adult brain, in particular if they are conserved in the primate brain.

Differentiated Cyno-1 ES Cells Did Not Form Teratomas

Both the cell-cycle length and the duration of the neurogenic period are considerably longer in primates than in rodents [23], and during primate cortical development there is acceleration of cell division (unlike in rodents). Whereas differentiated ES cells did not produce teratomas, continuous growth of grafted progenitors (normal for primate development) resulted in large neural grafts, as has been observed when grafting human fetal cortical and striatal (ganglionic eminence) cells into rats [33, 34]. Fetal human striatal progenitors display PCNA and Ki67 immunoreactivity 15–17 weeks post-transplantation. We have not observed cells derived from other germ layers, alkaline phosphatase activity, or expression of SSEA-4 in the grafts. In fact, our results in vivo are remarkably similar to those reported for fetal striatal human xenografts in terms of proliferation, neuronal and glial differentiation, maturation, and migration [35]. These results are consistent with previous studies using differentiated ES cells from mouse, primate, and human origin in transplantation experiments which have not reported teratoma formation [5–7, 11, 48,

49]. In previous experiments, the presence of proliferating precursors and rosette structures in vivo led us to modify our differentiation protocol and include a short pulse of mitomycin C before harvesting the cells; such modifications significantly reduced the graft size (supplemental online Fig. 2) and allowed for long-term follow-up in the present study. In experimental paradigms to investigate functional and morphological integration, treatment with mitomycin C can be useful.

Our study demonstrates long-term (>6 months) survival of grafted ES-derived neurons in an adult primate without immunosuppression, without adverse neurological or systemic effects. There was a remarkable similarity in cellular composition and distribution in the core of the grafts to that observed in grafts placed in rodents, where donor cells can be identified by expression of primate-specific markers. In the primate, more than 3,000 TH cells survived in the grafts. We observed signs of maturation in TH neurons such as DAT expression in TH-positive neurites. Primate DA neurons have a slower developmental and maturation rate than rodent neurons. In macaques, TH neurons are born between the fifth and sixth gestational weeks (E36-E42) and grow steadily during gestation (6 additional months) and first postnatal months until they reach mature size [50]. Nevertheless, maturation time may vary with culture conditions [32].

In summary, we demonstrate that following a stepwise approach in vitro mimicking developmental events, DA neurons derived from parthenogenetic primate ES cells can survive for long periods in the adult rodent and primate brain. Understanding and optimizing differentiation and cell selection for the specific purpose of therapeutic cell transfer will allow functional studies of these neurons for future application in Parkinson's disease and other neurodegenerative disorders.

REFERENCES

1 Thomson J, Itskovitz-Eldor J, Shapiro S et al. Embryonic stem cells derived from human blastocysts. Science 1998;282:1145–1147.

2 Cibelli JB, Grant KA, Chapman KB et al. Parthenogenetic stem cells in nonhuman primates. Science 2002;295:819.

3 Vrana KE, Hipp JD, Goss AM et al. Nonhuman primate parthenogenetic stem cells. Proc Natl Acad Sci U S A 2003;100(suppl 1):11911–11916.

4 Reubinoff BE, Pera MF, Fong CY et al. Embryonic stem cell lines from human blastocysts: somatic differentiation in vitro. Nat Biotechnol 2000;18:399–404.

5 Reubinoff BE, Itsykson P, Turetsky T et al. Neural progenitors from human embryonic stem cells. Nat Biotechnol 2001;19:1134–1140.

6 Kawasaki H, Suemori H, Mizuseki K et al. Generation of dopaminergic neurons and pigmented epithelia from primate ES cells by stromal cell-derived inducing activity. Proc Natl Acad Sci U S A 2002;99:1580–1585.

7 Zhang SC, Wernig M, Duncan ID et al. In vitro differentiation of transplantable neural precursors from human embryonic stem cells. Nat Biotechnol 2001;19:1129–1133.

8 Lee SH, Lumelsky N, Studer L et al. Efficient generation of midbrain and hindbrain neurons from mouse embryonic stem cells. Nat Biotechnol 2000;18:675–679.

9 Goridis C, Rohrer H. Specification of catecholaminergic and serotonergic neurons. Nat Rev Neurosci 2002;3:531–541.

10 Barberi T, Klivenyi P, Calingasan NY et al. Neural subtype specification of fertilization and nuclear transfer embryonic stem cells and application in parkinsonian mice. Nat Biotechnol 2003;21:1200–1207.

11 Kawasaki H, Mizuseki K, Nishikawa S et al. Induction of midbrain dopaminergic neurons from ES cells by stromal cell-derived inducing activity. Neuron 2000;28:31–40.

12 Ye W, Shimamura K, Rubenstein JL et al. FGF and Shh signals control dopaminergic and serotonergic cell fate in the anterior neural plate. Cell 1998;93:755–766.

13 Johe KK, Hazel TG, Muller T et al. Single factors direct the differentiation of stem cells from the fetal and adult central nervous system. Functions of basic fibroblast growth factor and neurotrophins in the differentiation of hippocampal neurons. Genes Dev 1996;10:3129–3140.

14 Sanchez-Pernaute R, Studer L, Bankiewicz KS et al. In vitro generation and transplantation of precursor-derived human dopamine neurons. J Neurosci Res 2001;65:284–288.

15 Bjorklund LM, Sanchez-Pernaute R, Chung S et al. Embryonic stem cells develop into functional dopaminergic neurons after transplantation in a Parkinson rat model. Proc Natl Acad Sci U S A 2002;99:2344–2349.

16 Mendez I, Hong M, Smith S et al. Neural transplantation cannula and microinjector system: experimental and clinical experience. Technical note. J Neurosurg 2000;92:493–499.

17 Abercrombie M. Estimation of nuclear populations from microtome sections. Anat Rec 1946;94:239–247.

18 Goridis C, Brunet J-F. Transcriptional control of neurotransmitter phenotype. Curr Opin Neurobiol 1999;9:47–53.

19 Echevarria D, Vieira C, Gimeno L et al. Neuroepithelial secondary organizers and cell fate specification in the developing brain. Brain Res Brain Res Rev 2003;43:179–191.

20 Ye W, Shimamura K, Rubenstein JL et al. FGF and Shh signals control dopaminergic and serotonergic cell fate in the anterior neural plate. Cell 1998;93:755–766.

21 Hynes M, Rosenthal A. Specification of dopaminergic and serotonergic neurons in the vertebrate CNS. Curr Opin Neurobiol 1999;9:26–36.

22 Simon HH, Bhatt L, Gherbassi D et al. Midbrain dopaminergic neurons: determination of their developmental fate by transcription factors. Ann N Y Acad Sci 2003;991:36–47.

23 Kornack DR, Rakic P. Changes in cell-cycle kinetics during the development and evolution of primate neocortex. Proc Natl Acad Sci U S A 1998;95:1242–1246.

24 Simerly C, Dominko T, Navara C et al. Molecular correlates of primate nuclear transfer failures. Science 2003;300:297.

25 Svendsen C, Caldwell M, Shen J et al. Long-term survival of human central nervous system progenitor cells transplanted into a rat model of Parkinson's disease. Exp Neurol 1997;148:135–146.

26 Ostenfeld T, Caldwell MA, Prowse KR et al. Human neural precursor cells express low levels of telomerase in vitro and show diminishing cell proliferation with extensive axonal outgrowth following transplantation. Exp Neurol 2000;164:215–226.

27 Yang M, Donaldson AE, Marshall CE et al. Studies on the differentiation of dopaminergic traits in human neural progenitor cells in vitro and in vivo. Cell Transplant 2004;13:535–547.

28 Winkler C, Fricker RA, Gates MA et al. Incorporation and glial differentiation of mouse EGF-responsive neural progenitor cells after transplantation into the embryonic rat brain. Mol Cell Neurosci 1998;11:99–116.

29 Fricker RA, Carpenter MK, Winkler C et al. Site-specific migration and neuronal differentiation of human neural progenitor cells after transplantation in the adult rat brain. J Neurosci 1999;19:5990–6005.

30 Galpern WR, Burns LH, Deacon TW et al. Xenotransplantation of porcine fetal ventral mesencephalon in a rat model of Parkinson's disease: functional recovery and graft morphology. Exp Neurol 1996;140:1–13.

31 Ben-Hur T, Idelson M, Khaner H et al. Transplantation of human embryonic stem cell-derived neural progenitors improves behavioral deficit in Parkinsonian rats. STEM CELLS 2004;22:1246–1255.

32 Takagi Y, Takahashi J, Saiki H et al. Dopaminergic neurons generated from monkey embryonic stem cells function in a Parkinson primate model. J Clin Invest 2005;115:102–109.

33 Grasbon-Frodl EM, Nakao N, Lindvall O et al. Phenotypic development of the human embryonic striatal primordium: a study of cultured and grafted neurons from the lateral and medial ganglionic eminences. Neuroscience 1996;73:171–183.

34 Grasbon-Frodl EM, Nakao N, Lindvall O et al. Developmental features of human striatal tissue transplanted in a rat model of Huntington's disease. Neurobiol Dis 1997;3:299–311.

35 Hurelbrink CB, Armstrong RJ, Dunnett SB et al. Neural cells from primary human striatal xenografts migrate extensively in the adult rat CNS. Eur J Neurosci 2002;15:1255–1266.

36 Holzschuh J, Hauptmann G, Driever W. Genetic analysis of the roles of Hh, FGF8, and nodal signaling during catecholaminergic system development in the zebrafish brain. J Neurosci 2003;23:5507–5519.

37 Hanashima C, Li SC, Shen L et al. Foxg1 suppresses early cortical cell fate. Science 2004;303:56–59.

38 Gunhaga L, Marklund M, Sjodal M et al. Specification of dorsal telencephalic character by sequential Wnt and FGF signaling. Nat Neurosci 2003;6:701–707.

39 Schuurmans C, Guillemot F. Molecular mechanisms underlying cell fate specification in the developing telencephalon. Curr Opin Neurobiol 2002;12:26–34.

40 Zappone MV, Galli R, Catena R et al. Sox2 regulatory sequences direct expression of a (beta)-geo transgene to telencephalic neural stem cells and precursors of the mouse embryo, revealing regionalization of gene expression in CNS stem cells. Development 2000;127:2367–2382.

41 Hitoshi S, Tropepe V, Ekker M et al. Neural stem cell lineages are regionally specified, but not committed, within distinct compartments of the developing brain. Development 2002;129:233–244.

42 Rousselot P, Lois C, Alvarez-Buylla A. Embryonic (PSA) N-CAM reveals chains of migrating neuroblasts between the lateral ventricle and the olfactory bulb of adult mice. J Comp Neurol 1995;351:51–61.

43 Doetsch F, Alvarez-Buylla A. Network of tangential pathways for neuronal migration in adult mammalian brain. Proc Natl Acad Sci U S A 1996;93:14895–14900.

44 Lois C, Garcia-Verdugo JM, Alvarez-Buylla A. Chain migration of neuronal precursors. Science 1996;271:978–981.

45 Kornack DR, Rakic P. Cell proliferation without neurogenesis in adult primate neocortex. Science 2001;294:2127–2130.

46 Whetton AD, Graham GJ. Homing and mobilization in the stem cell niche. Trends Cell Biol 1999;9:233–238.

47 Tsai RY, Kittappa R, McKay RD. Plasticity, niches, and the use of stem cells. Dev Cell 2002;2:707–712.

48 Kim JH, Auerbach JM, Rodriguez-Gomez JA et al. Dopamine neurons derived from embryonic stem cells function in an animal model of Parkinson's disease. Nature 2002;418:50–56.

49 Harper JM, Krishnan C, Darman JS et al. Axonal growth of embryonic stem cell-derived motoneurons in vitro and in motoneuron-injured adult rats. Proc Natl Acad Sci U S A 2004;101:7123–7128.

50 Levitt P, Rakic P. The time of genesis, embryonic origin and differentiation of the brain stem monoamine neurons in the rhesus monkey. Brain Res 1982;256:35–57.